Low-Loss Wide-FSR Miniaturized Racetrack Style Microring Filters for ⩾1 Tbps DWDM

Asher Novick,[1,*] Kaylx Jang,[1] Anthony Rizzo,[1] Robert Parsons,[1] and Keren Bergman[1]

[1] *Department of Electrical Engineering, Columbia University, New York, NY, 10027, USA*

[*] *asher.novick@columbia.edu*

Abstract: We demonstrate add-drop microring filters based on 180° varied-width hybrid Euler bends, suitable for supporting >Tbps DWDM. We measure FSR>40nm, 0.64nm/mW thermal tuning efficiency, and $IL_{off} \leqslant 0.02$dB across the C- and L-bands. © 2023 The Author(s)

1. Introduction

The rise of cloud-based computing and high-performance data analytic applications, such as machine learning, has strained traditional data center and high performance computing architectures. Silicon photonic (SiP) interconnect architectures have been proposed as a bandwidth-dense and energy efficient solution to the problem of bandwidth bottlenecks in these systems. For achieving SiP interconnects with >Tbps aggregate data rates, architectures utilizing on-chip dense wavelength division multiplexing (DWDM) with massive parallelism provide an appealing path forward [1]. Add-drop resonant filters, typically micro-ring resonators (MRRs) or disks, are ubiquitous in DWDM SiP interconnect architectures as compact, low-loss, and tunable wavelength-selective filters. By cascading multiple resonant filters along a single waveguide, de-multiplexing of independently modulated carrier frequencies to independent detectors is possible [1]. Thus, the maximum aggregate data bandwidth of such a receiver is the data rate per channel (Gbps/λ) multiplied by the number of wavelength channels (N_λ).

N_λ is dominated by three factors: minimum channel spacing ($\Delta\lambda_{aggressor}$), resonator free spectral range (FSR), and off-resonance insertion loss (IL_{off}). The feasibility of on-chip DWDM at 25 Gbps/λ for channel spacing as low as 100 GHz (≈ 0.8 nm in the C-band) with minimal inter-channel crosstalk penalties has been demonstrated [2]. FSRs as large as 93 nm have also been demonstrated, but such large FSRs are achieved at the cost of significant IL_{off} due to excess bend loss of the phase-matched coupling geometry that enables the requisite resonator coupling [3]. For a cascaded resonator array, cumulative IL_{off} will strongly impact the channel corresponding to the last resonator, limiting N_λ before a full FSR of optical bandwidth can be utilized.

Here, we demonstrate a miniaturized racetrack-style MRR filter based on a pair of single-mode 180° varied-width hybrid Euler bends. The devices were measured as having $FSR > 40$ nm, Lorentzian full-width half-max (FWHM) ≈ 50 GHz, and $IL_{off} \leqslant 0.02$ dB across the C- and L-bands, due to the straight coupling region. The thermal tuning efficiency was measured as 0.64 nm/mW. The same device is measured across 8 reticles over $\frac{1}{4}$ of a 300 mm wafer, showing the C-band resonance location varying with $1\sigma_{\lambda_0} = 1.1$ nm. To the best of our knowledge, this MRR supports the record for achievable $N_\lambda(IL_{limit} \leqslant 1\,\text{dB}, \Delta\lambda_{aggressor} \geqslant 0.8\,\text{nm}) = 50$, where IL_{limit} is the acceptable cumulative IL_{off}. As a result, a single array of these MRR filters, at 25 Gbps/λ, is capable of supporting an aggregate DWDM receiver bandwidth up to 1.25 Tbps.

2. Low-Loss MRR Design & Simulation for Large N_λ

The maximum N_λ is limited by two key MRR factors, FSR and IL_{off}, and can be calculated as,

$$N_\lambda = \text{floor}\left[\min\left(\frac{FSR}{\Delta\lambda_{aggressor}}, \frac{IL_{limit}}{IL_{off}} + 1\right)\right]. \tag{1}$$

$\min(\Delta\lambda_{aggressor})$ should be set proportional to the data rate, affecting the target MRR FWHM [2,4]. For feasible DWDM applications, an IL_{limit} must be defined as the maximum threshold for the broadband cumulative loss contributed by each MRR prior to the last channel in the system's cascaded array. We set our design $IL_{limit} = 1$ dB to reduce the range of expected signal quality across the spectrum. To increase N_λ, both ratios in Eq. 1 must be maximized, but prior works have focused on the former, $FSR/\Delta\lambda_{aggressor}$. This has been achieved via reducing the MRRs' effective radius R_{eff}, which is inversely proportional to FSR [3]. Yet, IL_{off} is equally important and often not reported; in the case of $IL_{off} = 0.1$ dB, $\max[N_\lambda(IL_{limit} = 1\,\text{dB})] = 11$, regardless of FSR.

Prior work suggests that the resonator's FWHM $\geqslant 2 \times$ Gbps/λ to avoid spectral truncation negatively impacting signal quality [4]. For 25 Gbps/λ this would correspond to FWHM $\geqslant 50$ GHz, which requires the resonator power coupling for the through and drop waveguides to be $\approx 5\%$ in the C-band (in the case of negligible resonator round trip loss). For ultra-wide FSR resonators, this coupling strength is typically achieved using a phase-matched directional coupler, partially wrapped around the resonator body, matching the resonator curvature and engineered to optimally couple into the resonator's fundamental optical mode [1, 3]. As a consequence, all of the light must pass through a pair of S-bends in the through waveguide, introducing significant IL_{off} losses through bend and mode mismatch losses at the straight-to-bent and concave-to-convex bent waveguide interfaces [5]. These losses scale exponentially with $1/R_{eff}$, thus the larger the FSR, the larger the IL_{off} for a phase-matched coupling scheme.

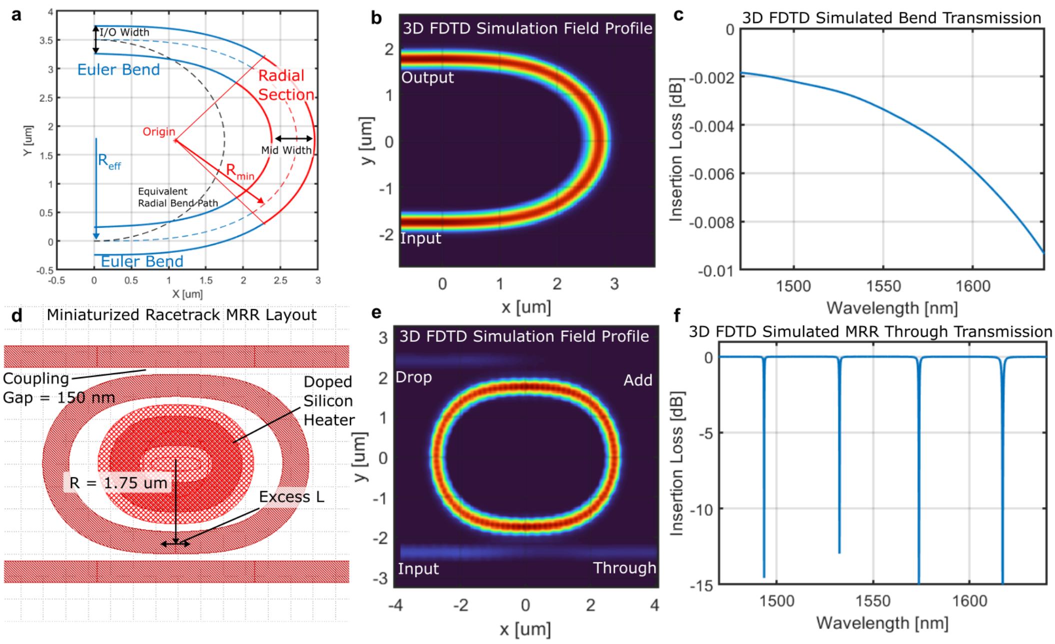

Fig. 1. **a)** 180° hybrid Euler bend with varied waveguide width, $R_{eff} = 1.75\,\mu$m, $R_{min} = 1.63\,\mu$m, I/O Width = 480 nm, and Mid Width = 577 nm. The blue sections illustrate where the waveguide curvature ($1/R$) and width linearly vary and red sections signify where waveguide curvature and width is constant. **b)** Simulated field profile of optical transmission through the 180° bend. **c)** Simulated $IL(\lambda)$/bend. **d)** Silicon layout of the miniaturized racetrack style MRR filter, with a ring shaped doped silicon heater included for thermally tuning the resonance location via the thermo-optic effect. Excess straight waveguide is added between the 180° bends to adjust the nominal resonance location. **e)** Simulated field profile of the MRR, with the fundamental mode launched from the input port. **f)** Simulated MRR $IL(\lambda)$ measured at the through port.

To overcome this, we propose utilizing a pair of 180° modified hybrid Euler bends (comprised of concatenated Euler and radial bends with varied-width), illustrated in Fig. 1a, to construct a MRR [6]. Figs. 1b and 1c show the FDTD simulation field profile and transmission of the bend measured from input to output, with less than 0.01 dB/bend at $R_{eff} = 1.75\mu$m. The resulting MRR, shown in Fig. 1d, is quasi-ellipsoidal, with an approximately linear region at the top and bottom. This geometry permits an extended linear coupling region, similar to a larger race-track style MRR. Removing the tight S bends from the through waveguide also removes the off-resonance bend and mode mismatch losses, drastically reducing IL_{off}. Figs. 1e and 1f illustrate the FDTD simulations for this MRR, which are in good agreement with our expectation of low IL_{off} and FSR$>$ 40nm.

3. Experimentally Measured MRR Characteristics

MRRs were fabricated with the excess length varied from 0 to 250 nm and their measured normalized through port transmission is plotted in Fig. 2a, showing consistent critical coupling, FSR $>$ 40 nm, and FWHM $\approx$ 50 GHz for each variation. The thermal tuning efficiency is measured as 0.63 nm/mW, shown in Fig. 2b, and a single MRR variation ($L = 0$) is measured on 8 reticles, sampled across $\frac{1}{4}$ of a 300 mm diameter wafer, as having a $1\sigma_{\lambda_0} = 1.1$ nm variation in resonance location. This suggests 99.7% of fabricated devices should fall within ± 3.3 nm of the nominal target λ_0, and the average per device thermal tuning energy $P_{\text{th}} = 5.24$ mW to compensate for fabrication variation (210 fJ/bit at 25 Gbps/λ). A series of cascaded resonator cutback measurements of both the proposed MRR with linear coupling and a resonator with a phase-matched coupling scheme confirms the former results in reducing IL_{off} by more than a factor of 4 over the full C- and L-bands, as seen in Fig, 2d. The resonator with the phase-matched coupler also has a 63% lower FSR, corresponding to a much larger R_{eff} and lower bend losses. We extrapolate that for equivalent FSR resonators, our IL_{off} improvement relative to a phase-matched coupler geometry would be much greater than the factor of 4 measured here.

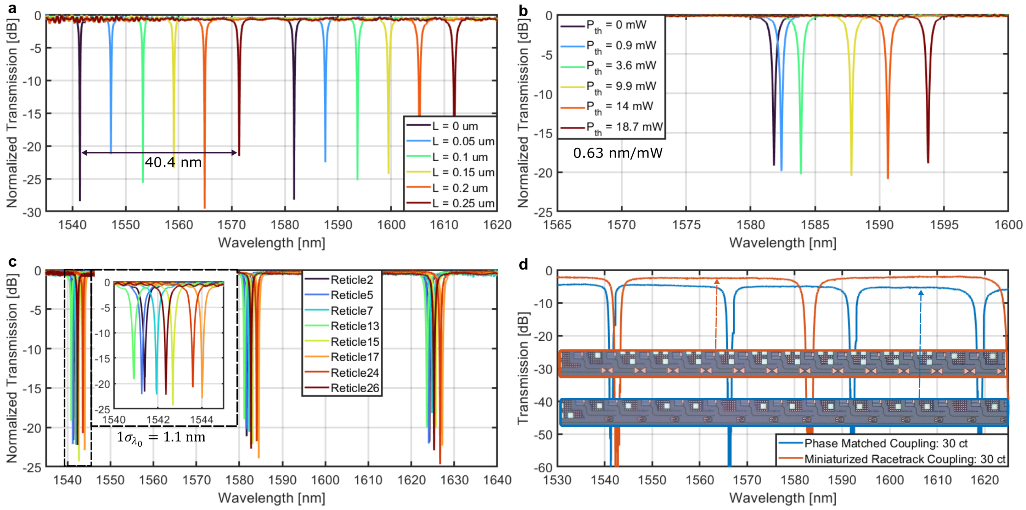

Fig. 2. **a)** Measured transmission of multiple MRRs with the L parameter varied to adjust nominal resonance wavelengths. FWHM $\approx 50\,$GHz, with negligible change over $0 < L < 0.25\,\mu$m. **b)** Thermal tuning response using the integrated heater, as shown in Fig.1d, tuning efficiency measured as 0.63 nm/mW. **c)** Variation of the same device over multiple reticles, sampled across $\frac{1}{4}$ of a 300 mm wafer. $1\sigma_{\lambda_0} = 1.1\,$nm. **d)** Subset of the cutback measurements made for different resonators. 30 cascaded MRRs with a bent phase-matched coupler ($R_{\mathrm{MRR}} \approx 4.4\,\mu$m) show $IL_{off} \approx 0.09\,$dB, compared to our miniaturized racetrack coupled MRR, which shows $IL_{off} \leq 0.02\,$dB. Insets are microscopic images of adjacent cascaded resonator arrays.

4. Conclusion

We design and experimentally demonstrate an add-drop MRR filter capable of supporting up $\geqslant$ 1 Tbps along a single cascaded resonator array. To the best of our knowledge, the MRR demonstrated in this work is capable of supporting the largest feasible N_λ, as well as the largest feasible aggregate bandwidth, for a single array of cascaded add-drop MRR filters. This work supports the next generation of energy-efficient and bandwidth dense on-chip DWDM interconnects.

References

1. A. Rizzo, S. Daudlin, A. Novick *et al.*, "Petabit-scale silicon photonic interconnects with integrated kerr frequency combs," IEEE J. Sel. Top. Quantum Electron. **29**, 1–20 (2022).
2. H. Jayatilleka *et al.*, "Crosstalk in soi microring resonator-based filters," J. Light. Technol. **34**, 2886–2896 (2016).
3. D. Liu, C. Zhang, D. Liang, and D. Dai, "Submicron-resonator-based add-drop optical filter with an ultra-large free spectral range," Opt. Express **27**, 416–422 (2019).
4. Y.-H. Hung *et al.*, "Silicon photonic switch-based optical equalization for mitigating pulsewidth distortion," Opt. Express **27**, 19426–19435 (2019).
5. J. H. Song *et al.*, "Low-loss waveguide bends by advanced shape for photonic integrated circuits," J. Light. Technol. **38**, 3273–3279 (2020).
6. F. Vogelbacher *et al.*, "Analysis of silicon nitride partial euler waveguide bends," Opt. Express **27**, 31394–31406 (2019).

Acknowledgements: This work was supported in part by the U.S. Defense Advanced Research Projects Agency under PIPES Grant HR00111920014 and in part by the U.S. Advanced Research Projects Agency–Energy under ENLITENED Grant DE-AR000843. The wafer/chip fabrication and custom device processing were provided by AIM Photonics/SUNY Poly Photonics engineering team and fabricator in Albany, New York

Disclaimer: Preliminary paper, subject to publisher revision